On the Need to Modify the Sea Surface Roughness Formulation over Shallow Waters

PEDRO A. JIMÉNEZ

Research Applications Laboratory, National Center for Atmospheric Research, Boulder, Colorado

JIMY DUDHIA

Mesoscale and Microscale Meteorology Laboratory, National Center for Atmospheric Research, Boulder, Colorado

(Manuscript received 19 May 2017, in final form 1 March 2018)

ABSTRACT

The wind stress formulation in an atmospheric model over shallow waters is investigated using year-long observations of the wind profile within the first 100 m of the atmosphere and mesoscale simulations. The model experiments use a range of planetary boundary layer parameterizations to quantify the uncertainty related to the turbulent closure assumptions and thus to isolate the dominant influence of the surface roughness formulation. Results indicate that a positive wind speed bias exists when common open-ocean formulations for roughness are adopted for a region with a water depth of 30 m. Imposition of a wind stress formulation that is consistent with previous shallow-water estimates is necessary to reconcile model wind speeds with observations, providing modeling evidence that supports the increase of surface drag over shallow waters. The possibility of including water depth in the parameterization of roughness length is examined.

1. Introduction

The roughness of the ocean is mainly controlled by the wave field, which is in turn determined to a large extent by the wind (Edson et al. 2013). In general, the ocean surface is rougher for increasingly higher winds. Over the open ocean, a modified version of the Charnock relationship (Charnock 1955) provides a good representation of the feedback between the wind speed and the surface roughness (Edson et al. 2013). Data from field campaigns such as the Humidity Exchange over the Sea (HEXOS) program (DeCosmo et al. 1996; Janssen 1997) have revealed that, over shallow waters, the roughness of the surface is higher than the corresponding values over the open ocean (Geernaert et al. 1986, 1987; Smith et al. 1992; DeCosmo et al. 1996; Taylor and Yelland 2001), however. Despite this differentiated observed behavior, atmospheric models apply the same wind stress formulation regardless of the depth of the waters.

Here we show that a significant wind speed bias exists when comparing model results using wind stress formulations valid for the open ocean with wind profile data over the first 100 m of the atmosphere in shallow waters and that increasing the surface roughness length is sufficient to reconcile model results with the observed wind profile. We focus on just one aspect—depth—of the complex problem related to drag over shallow-water surfaces. We do not consider other aspects, such as fetch or wave age, that modulate the drag over shallow waters (e.g., Mahrt et al. 1996; Fairall et al. 2006; Vickers and Mahrt 2010; Grachev et al. 2011). Traditional formulations also do not consider fetch or wave age and represent an average over all conditions (e.g., Charnock 1955; Edson et al. 2013). Our results, fitting long-term wind measurements that in turn provide good agreement with theoretical findings, provide modeling evidence that supports the increase of the ocean roughness found in field campaigns and demonstrate the necessity of introducing a representation of the wind stress over shallow waters that differs from the one that is used over the deeper ocean.

2. Observational evidence

Observational evidence indicates that the surface drag over the ocean is a positive function of the wind speed

Corresponding author: Pedro A. Jiménez, jimenez@ucar.edu

DOI: 10.1175/JAMC-D-17-0137.1

(Jones and Toba 2001; Bryant and Akbar 2016). Using nondimensional arguments, Charnock (Charnock 1955) postulated that roughness length z_0 is proportional to the square of the friction velocity u_*:

$$z_0 = (a/g)u_*^2, \tag{1}$$

where g is the gravitational acceleration and the factor a is an empirical constant known as the Charnock parameter. Subsequent field experiments have reported a range of values for the parameter (Geernaert et al. 1986; Kitaigorodskii and Volkov 1965; Wu 1982; Garratt 1977). More-recent empirical evidence suggests a dependence of the Charnock parameter on the wind speed (Edson et al. 2013; Fairall et al. 2003) or even on the sea state (Smith et al. 1992; Fairall et al. 2003; Donelan 1990; Oost et al. 2002). Nowadays, the Coupled Ocean–Atmosphere Response Experiment (COARE) algorithm provides one widely used relationship (Foreman and Emeis 2010). Satisfactory agreement over the open ocean within the framework of the COARE algorithm has recently been found using a Charnock parameter that is a function of the wind speed (Edson et al. 2013).

There is agreement that over shallow waters the sea is rougher than over the open ocean for a given wind speed (Geernaert et al. 1986, 1987; Smith et al. 1992; DeCosmo et al. 1996; Taylor and Yelland 2001; Foreman and Emeis 2010). The added drag over shallow waters is increasingly larger for higher winds in comparison with the values over the open ocean. The physical mechanism responsible for this effect is unclear, but it has been speculated to be associated with either 1) the effects of the ocean bathymetry, whereby relatively shallow water slows the phase speed of the waves, which then become shorter and steeper in an effect known as shoaling (Foreman and Emeis 2010), or 2) form drag due to short (young) waves (DeCosmo et al. 1996). Taylor and Yelland (2001) have identified the steepness H/L as the main parameter for roughness, rather than just wave height (L is the dominant wavelength). In shoaling, H stays more or less constant (as long as the depth is still much greater than H) while L decreases (the wave period is conserved). This situation means that H/L increases, which means more drag. They showed that this collapses a variety of datasets with different depths onto each other. Despite the different properties of the sea surface, regional and global atmospheric models (e.g., ECMWF and GFS) widely use a roughness formulation such as Eq. (1) with a Charnock parameter that is valid for the open ocean. We will show that models using the standard formulation are systematically overestimating the lower-level winds over regions with shallow waters; we hypothesize that it is because the drag over these regions should be higher in comparison with the open ocean, especially for higher wind speeds, when accounting for shallow-water effects.

3. Numerical evidence

a. Experimental setup

We have performed a series of modeling experiments with version 3.5.1 of the Weather Research and Forecasting (WRF) Model (Skamarock et al. 2005). To obtain statistically robust conclusions, we simulated the atmospheric evolution over a coastal region during a complete year wherein observations of the wind speed were available at a total of eight levels within the first 100 m of the atmosphere (i.e., 33, 40, 50, 60, 70, 80, 90, and 100 m). The observations were acquired at the research platform FINO1 (FINO comes from Forschungsplattformen in Nord- und Ostsee), which is located approximately 48 km from the German coast (54.01°N, 6.59°E) with a depth of about 30 m. Quality control was applied to the 10-min-averaged data following ideas described in Jiménez et al. (2010). The quality-controlled wind speed data were subsequently hourly averaged, completing the data-preparation process. The year of 2009 was selected because of the availability of data at all of the levels and 2009's near-climatological wind conditions. The predominant winds in 2009 are therefore from the southwest, which minimizes disturbances that result from shadowing of the tower. The prevailing winds are also not affected by the installation of wind turbines to the east of FINO1 during the second half of 2009. Hence, potential disturbances associated with the wind turbines are of small magnitude given the climatological character of this work.

The physical and dynamical settings used in the WRF simulations are essentially the same as those used in previous studies (Jiménez et al. 2009, 2011a,b), the only difference being the addition of five vertical levels near Earth's surface that have been shown to reproduce the wind speed profile over land (Jiménez et al. 2016). The model is initialized at 0000 UTC of each day and run for 48 h, recording the output every hour. The first day is discarded as a spinup of the model, and the second day is retained as the simulation for that day. The process is repeated until a simulation for each day of 2009 is obtained. Data from ERA-Interim (Dee et al. 2011) are used as initial and boundary conditions. Sensitivity experiments were performed on the horizontal resolution. Different simulations for the complete year of 2009 were performed at 27, 9, and 3 km (Fig. 1), with very little sensitivity in the wind speed distribution, and therefore the simulations herein presented were performed over a single domain of 27-km horizontal resolution. The domain covers the complete North Sea and the eastern

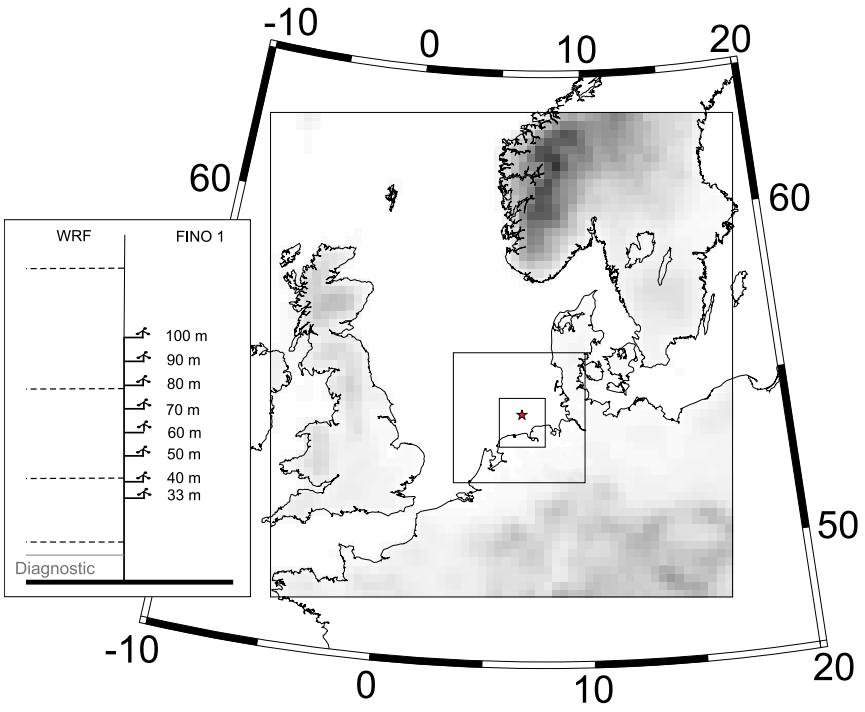

FIG. 1. The three domains of 27-, 9-, and 3-km horizontal resolution and the location of FINO1 (star). The vertical distribution of the levels closer to the surface is also shown (inset).

part of the Baltic Sea. A total of 36 vertical levels were used in the vertical direction, with 5 of them within the first 200 m of the atmosphere (i.e., 15, 40, 80, 140, and 200 m). Tests showed that this number of levels is adequate to resolve the tower profile layer and that, with the lowest level nearer 15 m than 30 m, the results are robust to its variation.

Realizing the possible sensitivity of the wind profile to the closure assumptions associated with the representation of the turbulent mixing within the planetary boundary layer (PBL), we used four different PBL parameterizations (Hong et al. 2006; Pleim 2007; Nakanishi and Niino 2009; Bretherton and Park 2009) in each experiment to quantify this part of the uncertainty. The first one imposes the shape of the vertical profile of the eddy diffusivities (K-profile method) in a first-order closure (Hong et al. 2006). The second one is based on a combination of a transilient approach with a local scheme and is also a first-order closure (Pleim 2007). The third and fourth parameterizations impose a 1.5-order closure that resolves the turbulent kinetic energy equation to compute the eddy diffusivities (Nakanishi and Niino 2009; Bretherton and Park 2009). These last two parameterizations mainly differ in the formulation of the turbulent length scale. This experimental design allows us to quantify the uncertainty related to the turbulent closure to isolate the effects of the roughness formulation.

b. *Sensitivity to the wind stress formulation*

To avoid the influence of timing errors in the simulations that would bias short-lived low- and high-wind events, we focus on the wind speed distribution characteristics (represented with 99 percentiles) only. The comparison of the observed and simulated wind speed distributions calculated with data corresponding to the 8760 h of 2009 is shown, for the sensor located at 60 m (one of the middle sensors), as a percentile–percentile comparison (Wilks 1995) in Fig. 2 (red area). The simulated wind at the nearest grid point to FINO1 is used in the comparison. The modeling results clearly indicate a progressive overestimation of the frequency of moderate–high wind speeds. Data from all sensors are in close agreement with this finding. The systematic overestimation for all formulations of the turbulent mixing points to limitations in the representation of the ocean–atmosphere interactions as a potential source of the discrepancies. Indeed, the overestimation can be understood in terms of the z_0 formulation used by WRF, which consists of a Charnock relationship that follows Eq. (1) with $a = 0.0185$ (Wu 1982), consistent with values observed over the open ocean. Assumption of a linear dependence of the Charnock parameter with the

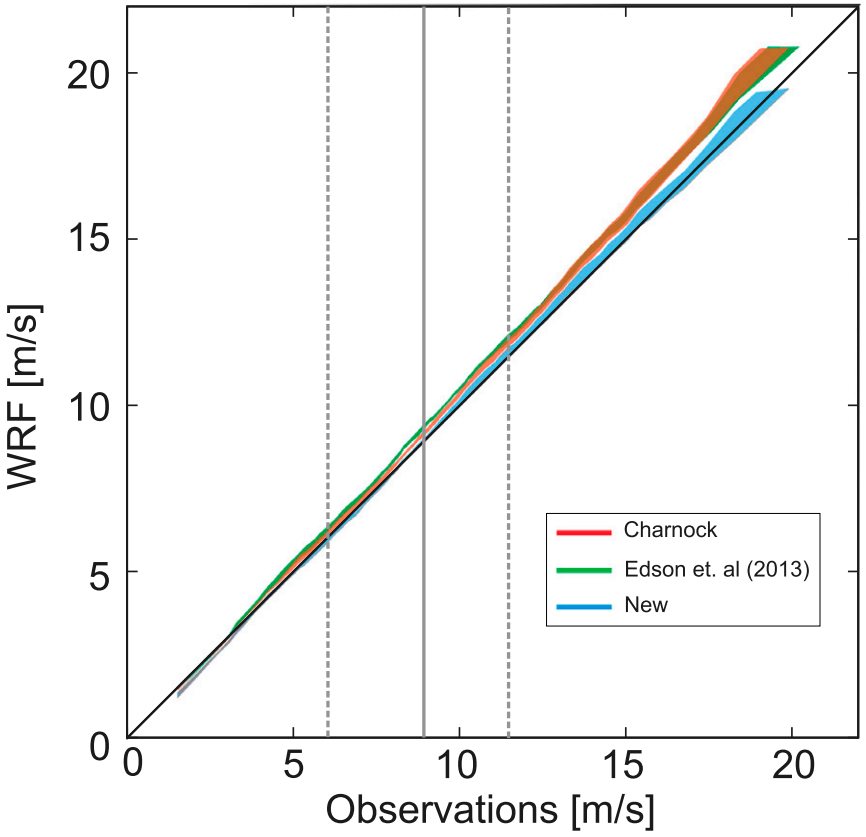

FIG. 2. Percentile–percentile plot of the observed and simulated wind speed. Each of the simulated percentiles (from 1% to 99%) is plotted against its associated observed percentile, and the absolute range of the percentiles from the four different turbulence closures of each WRF experiment is shaded. The colors indicate the WRF experiment (see legend): red is the standard WRF formulation, green is the ocean roughness formulation for the open ocean from the COARE algorithm (Edson et al. 2013), and blue is the alternative formulation herein presented [Eq. (3)]. The solid gray vertical line represents the median of the observations, and the dashed gray lines represent the 25th and 75th percentiles.

wind speed ($a = 0.0017u_{10} - 0.005$, where u_{10} is the wind speed at 10 m above the surface), as reported to be more valid over the open ocean by the COARE algorithm (Edson et al. 2013), shows a small sensitivity relative to the previous estimation (green; Fig. 2). In particular, this second experiment also overestimates the frequency of moderate–high winds.

These findings support our working hypothesis that the wind speed over shallow waters will be overestimated and therefore indicate the necessity of improving the representation of the ocean roughness over these regions. To reinforce this statement further, Fig. 3a shows the drag coefficient C_d (u_*^2/u_{10}^2). The symbols represent observations recorded during the international HEXOS program (Janssen 1997) that took place in the vicinity of the Dutch Noordwijk platform (52.27°N, 4.30°E) with 18 m of ocean depth. HEXOS data have been used because of the quality of the measurements and their relatively close proximity to FINO1. The C_d values as a result of assuming a neutral atmosphere and the standard WRF formulation (red line) are in closer agreement with the open-ocean formulation from the COARE algorithm (green line) than with the shallow-water data from the HEXOS program (symbols). In particular, the drag is underestimated by both formulations for moderate–high winds, supporting our previous expectations. Similar comments can be made for the friction velocity (Fig. 3b), which shows how the two formulations (green and red lines) are in agreement with the lower part of the observational scatter with a clear underestimation of the recorded values at moderate–high winds.

To provide complementary evidence of the importance of the roughness formulation, we have performed additional WRF experiments for 2009 for various fixed

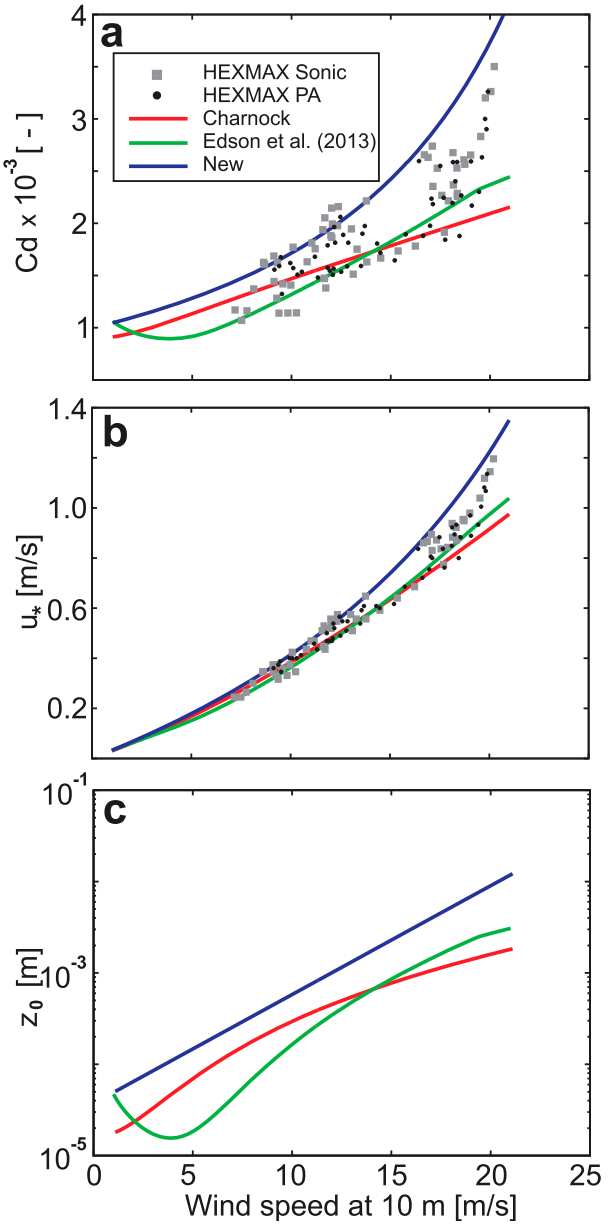

FIG. 3. (a) Drag coefficient, (b) friction velocity, and (c) roughness length as a function of the 10-m wind speed for the three different formulations of the ocean roughness (see legend). The symbols in (a) and (b) show the data recorded during the Humidity Exchange over the Sea Main Experiment (HEXMAX), a field experiment of the HEXOS program (Janssen 1997). The squares are the data recorded with a sonic anemometer, whereas the circles were recorded with a pressure anemometer.

roughness lengths (not shown) and then modified the z_0–wind relation to suppress the wind speed biases over the full range. The new formulation assumes that the logarithm of the surface roughness is a linear function of the wind speed at the first model level (15 m; u_{15}):

$$\log_{10}(z_0/z_{1\mathrm{m}}) = 0.125u_{15} - 4.5, \tag{2}$$

where $z_{1\mathrm{m}}$ is 1 m. The z_0 values are consistent with the previous experiments for low winds but reach significantly higher values for moderate–high winds (Fig. 3c). A value of 0.01 m is reached at 20 m s^{-1}, giving a 10-m drag coefficient of greater than 0.003 (blue line in Fig. 3a), which would be considered high for a deep-water surface even in conditions of strong wind. The parameters in the linear relationship have been selected in such a way that this third WRF experiment is successful in reducing the bias over the full range (blue shading in Fig. 2). From a modeling perspective, it is better to introduce a relationship between z_0 and u_* to remove height dependence and to add stability effects. If we assume a logarithmic wind profile that is typical of neutral conditions and substitute the wind speed with the one provided by the linear function [Eq. (2); blue line in Fig. 3c], we obtain

$$\ln\left(\frac{z_0}{z_{1\mathrm{m}}}\right) = \frac{(2.7u_* - 14.4)}{(u_* + 1.39)}, \tag{3}$$

which is now a stability-dependent formula imposed in the new WRF experiment. We will show in section 4 that this equation is supported by the theory of Taylor and Yelland (2001). The assumption of a neutral atmosphere is a good approximation given the larger impact of the new formulation for moderate–high winds when the atmosphere is nearly neutral. Hence, the effects of atmospheric stability are included through u_*. The u_* values obtained with this new formulation are also shown in Fig. 3b (blue line). The new formulation is in better agreement with the shape of the HEXOS data, capturing the increase of the ocean roughness observed over shallow waters, although it tends toward higher values. This result confirms that increasing the z_0 values over shallow waters is necessary and sufficient to remove the overestimation of the intensity of moderate–high wind events by models (blue shading in Fig. 2).

To test the effect of this change on the profile for various stability conditions, we show further in Fig. 4 the deviations from the percentiles calculated with observations for this new experiment and the experiment using the standard WRF formulation. Stability is determined with the simulated stability parameter z/L, where z is the height of the first model level, the surface layer, and now L is the Obukhov length. The results using the new formulation (Fig. 4b) are clearly in better agreement with observations than the standard formulation (Fig. 4a) is at the three vertical levels shown. The rest of the heights with wind records available show virtually the same results, indicating that increasing z_0

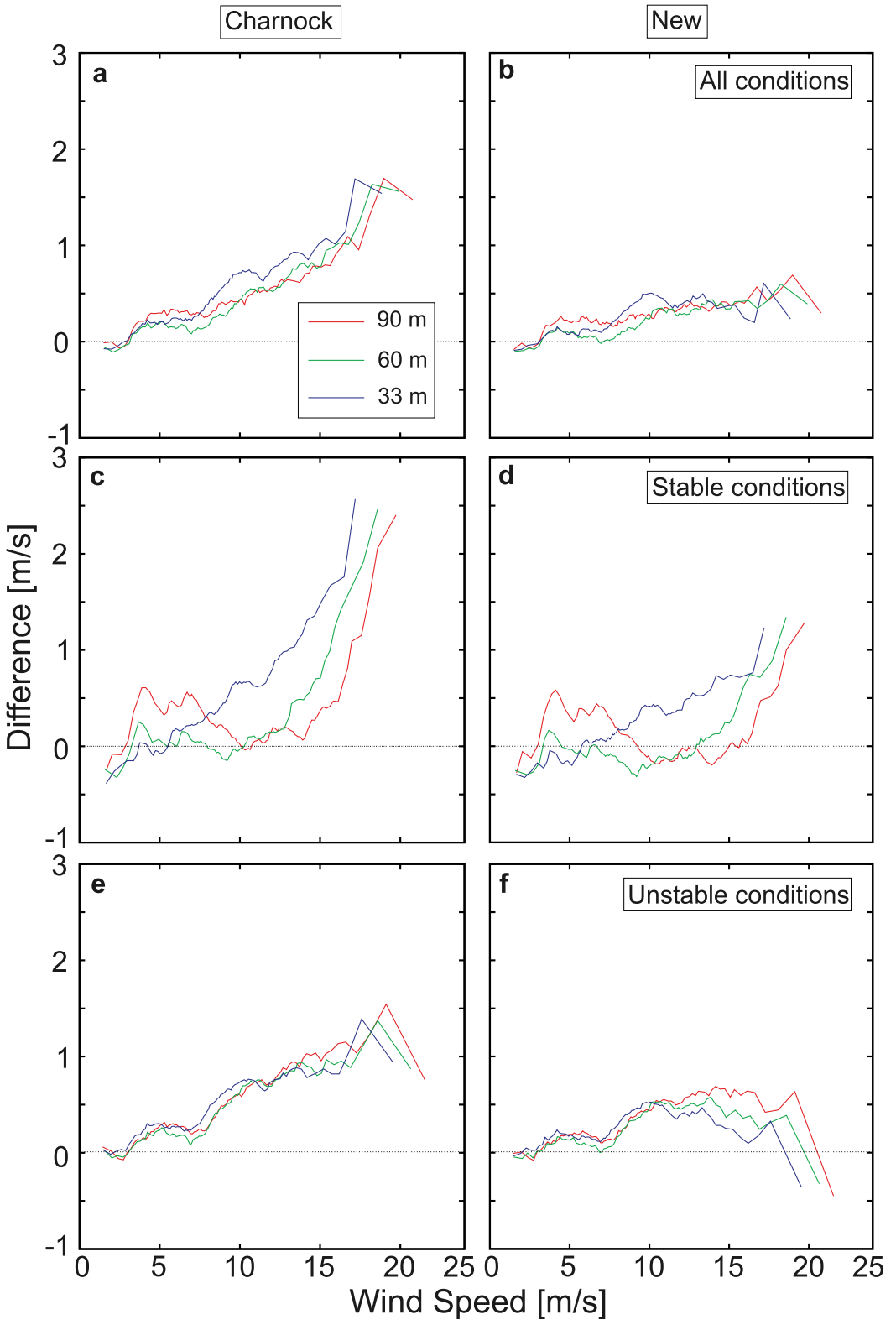

FIG. 4. Difference between the observed and simulated wind speed percentiles (from 1% to 99%) vs the observed wind speed for (left) the standard WRF experiment and (right) the one using the shallow-water formulation [Eq. (3)]: (a),(b) all of the dataset, (c),(d) stable conditions, and (e),(f) unstable conditions. The data used for each experiment are the average of the four simulations using the different parameterizations of the turbulence mixing. Results for three heights are shown (30, 60, and 90 m; see legend).

improves the simulated replication of the whole observed wind profile. Figures 4c and 4d show the deviations in the subset for stable conditions, and Figs. 4e and 4f show the deviations for unstable conditions. The overestimation of the high-wind frequency is improved under both atmospheric stability conditions, further reinforcing the attribution of the overestimation to the ocean–atmosphere interactions. It is noted that the previous high-wind overestimation was especially strong in stable conditions, and this was corrected well.

An idealized WRF numerical experiment (not shown) has ruled out the possibility that the sea roughness is influenced by the wind direction at FINO1. In this direction, it could have been argued that southerly winds approaching FINO1 from shallower waters have a different roughness than northerly winds. Our idealized WRF experiment indicated that the wind adjusts to a 10-fold roughness-length step within a few tens of kilometers, however. The idealized experiment imposes constant initial wind and a surface heterogeneity representing a portion of ocean, and it uses a grid spacing of 4 km. Both the wind speed and the friction velocity present a relatively abrupt change at the heterogeneity. The influence of the heterogeneity becomes negligible within a few tens of kilometers, however. Our simulations use a grid spacing of 27 km, which indicates that the impact of the heterogeneity at the coast is small. The small impact of this kind of representativeness issue is also supported by the nearby bathymetry, which is not too variable, especially in the dominant wind direction.

4. Generalized formulation

Our results constitute a starting point toward a better representation of the ocean–atmosphere interactions in atmospheric models. In this direction, inclusion of ocean bathymetry as static input data can be used to discern the formulation used to represent the ocean roughness, and depth can become a parameter of the roughness representation since the drag coefficient has been shown to increase for increasingly shallower waters (e.g., Taylor and Yelland 2001). For instance, Taylor and Yelland's Fig. 4b indicates that the wind behavior goes approximately linearly with the logarithm of the depth and that, by a depth of 100 m, the depth effect should collapse to the deep-water value for winds up to 20 m s^{-1}. To add the depth effect to our formulation, we chose to vary the linear gradient in Eq. (2) according to a logarithmic function of depth. At 30-m depth the gradient that we denote as b is equal to 0.125 s m^{-1}, which coincides with the fitted parameter in Eq. (2). The value of b decreases with increasing depth d as $b = (1/30)\ln(1260/d)$ and becomes 0.084 s m^{-1} at 100 m. This value provides a close fit to the Charnock relation, and so we

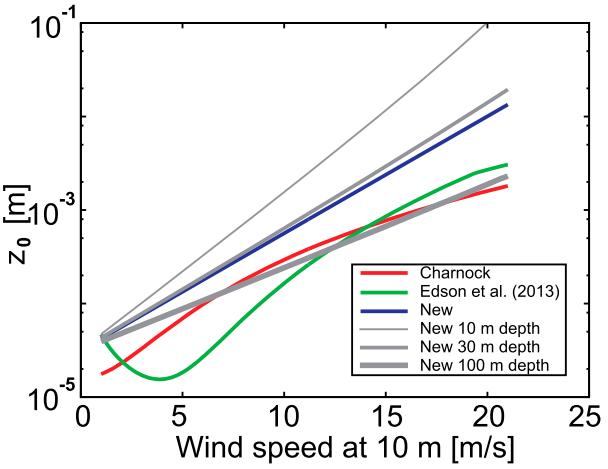

FIG. 5. Roughness length as a function of the 10-m wind speed for different formulations of the ocean roughness (see legend).

cap the value of depth at 100 m. At 10-m depth, $b = 0.161$ s m^{-1}, but for strong winds the roughness length becomes high and we would recommend capping it at $z_0 = 0.1$ m, corresponding to $C_d > 0.007$ when the wind slightly exceeds 20 m s^{-1}. We do not expect the relation to hold well for a depth of less than 10 m, because the depth and wave height become comparable, leading to very nonlinear behavior, and we would use 10 m as a minimum. The generalized formula replacing Eq. (3), including depth and limited to between 10 and 100 m, becomes

$$\ln\left(\frac{z_0}{z_{1\mathrm{m}}}\right) = \frac{(2.7u_* - 1.8/b)}{(u_* + 0.17/b)}. \tag{4}$$

The equation is therefore in agreement with our findings at 30 m and with the Charnock relation for deep water (Fig. 5). In addition, Eq. (4) is in agreement with the Taylor and Yelland (2001) theory at other depths. This result is illustrated in Fig. 6, which shows the normalized drag as a function of water depth and wind speed. Figure 6 is in good agreement with equivalent results from the Taylor and Yelland (2001) theory (their Fig. 4b). The good agreement provides theoretical support to our Eq. (4) since Taylor and Yelland (2001) have shown how their theory collapses a variety of observational datasets with different depths onto each other. The performance of Eq. (4) should be examined with numerical experiments and long-term observations at different depths.

5. Independent testing

To further examine the validity of our findings, we performed additional testing of our formulations [Eqs. (3) and (4)] at an independent observational site. The site is FINO3 located in the North Sea to the west of

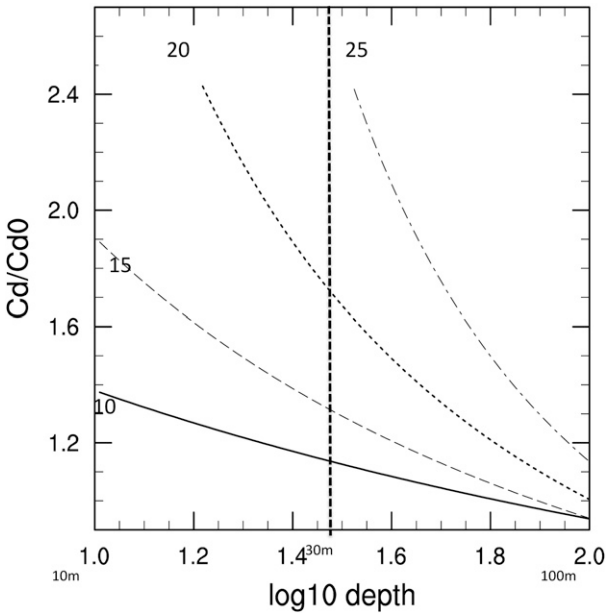

FIG. 6. Normalized drag vs depth for different wind speeds calculated with Eq. (4). The drag is normalized by the Charnock relation.

Denmark (55.20°N, 7.16°E), with a depth of about 22 m. Although this depth is close to the ocean depth at FINO1 (30 m), the site is selected because of the availability of long-term records of the wind speed at a total of nine levels (i.e., 30, 40, 50, 60, 70, 80, 90, 100, and 109 m).

Three WRF simulations were performed with the same WRF configuration as the one used at FINO1 (section 3a). The only difference between the experiments is the sea surface roughness representation. The first experiment uses the Charnock relation that is valid for the open ocean. The second experiment imposes the shallow-water formulation identified at FINO1 [Eq. (3)]. The third experiment uses our generalized Eq. (4) with the water depth set to the FINO3 depth (i.e., 22 m). The simulations for the three experiments span 2010. This year was selected because of the good data availability and its climatological wind behavior. The three experiments parameterize the turbulent mixing with the Yonsei University PBL option. The data preparation to compare the simulations with observations is the same as the one performed at FINO1 (section 3a).

Results are summarized with the percentile–percentile comparison at three vertical levels in Fig. 7. The simulation using the Charnock relation clearly overestimates the frequency of high wind speeds at the upper six of the nine anemometers (above 50 m; e.g., Figs. 7a,b). This result is consistent with findings at FINO1, revealing that the model tends to have a high bias with the deep formulation and further suggesting the necessity to review

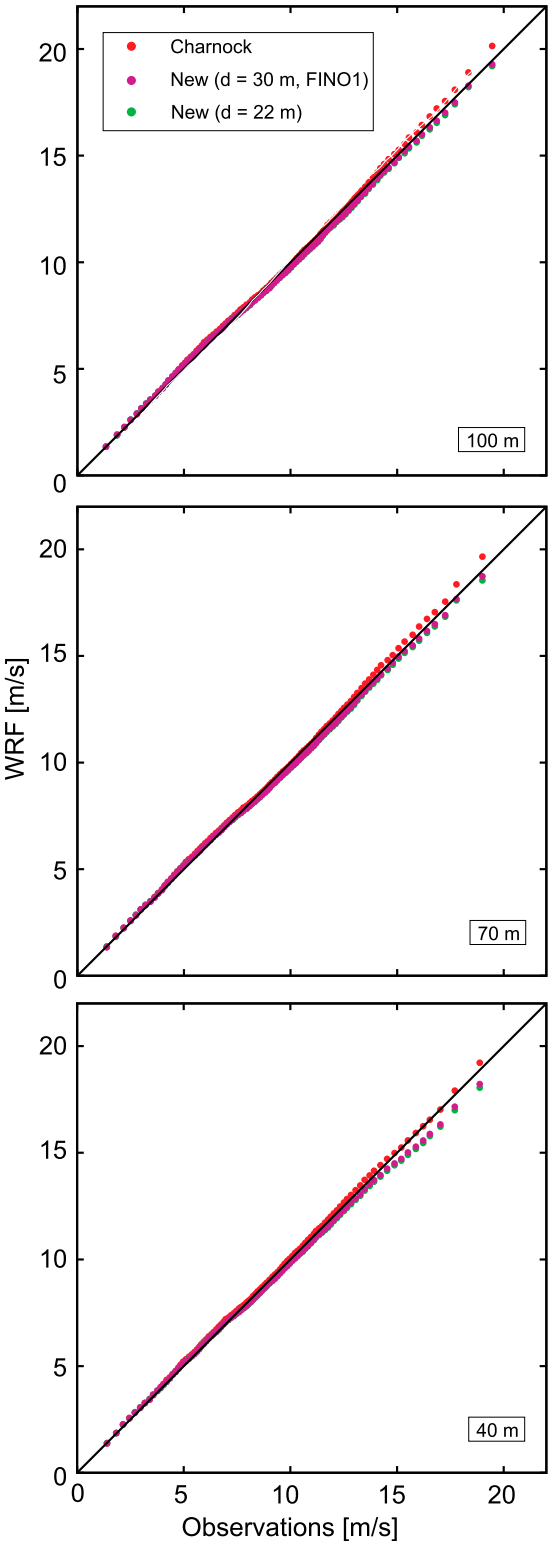

FIG. 7. Percentile–percentile plot of the observed and simulated wind speed at FINO3: (a) 100, (b) 70, and (c) 40 m. The colors represent results for different sea surface roughness formulations (see legend).

the ocean drag formulation over shallow waters. When we replace the ocean drag relationship with our equations for shallow waters [Eqs. (3) and (4)], the simulations provide a better fit to the wind speed distribution at the six uppermost anemometers (e.g., Figs. 7a,b). Although FINO3 nominal depth is 22 m, the results indicate that it behaves more like 30 m (the same as FINO1) possibly because much of the nearby area, especially to the west, is closer to 30 m. The lower two anemometers (up to 40 m) tend to behave better with the deep-water formulation, but it is not clear why because FINO1 was improved at all levels. Nevertheless, we view this as an improvement, especially for the levels above 50 m that is relevant to wind-energy applications, for example.

6. Conclusions

Our findings present modeling evidence that supports the increase of the surface drag over shallow waters in comparison with the standard formulation derived from observations over the open ocean. Results presented herein are valid for wind speeds up to 20 m s^{-1}. There is an increase of drag at the location of FINO1 of about 30%, and this magnitude should be relevant to forcing of the ocean in coupled models. We are confident in generalizing the validity of the results given the length of the simulated period (1 yr) and the consistency found between the eight vertical levels at FINO1. Anyway, results from this work should be confirmed by independent observations given the poor documentation of the data recorded at FINO1. In this direction, our findings support the FINO1 observations since the model agrees well with the data at all heights. The independent experiments at FINO3 also support our findings of the biases of the standard formulation at FINO1 and show an almost similar improvement with our new shallow-water roughness formulation.

Our method to examine consistency between modeled winds and observations differs from the standard approach. The standard practice is to fit a wind stress equation to existing observations (e.g., Andreas et al. 2012; Edson et al. 2013) and to impose this parameterization in the models. Herein we identified a wind stress formulation that suppresses the wind speed bias, and we subsequently compare this parameterization with wind stress observations. This alternative method only uses long-term wind speed measurements to improve the parameterization, which may be a more direct and robust approach that also statistically captures a representative sample of wind-sea states.

We have explored the possibility of using a depth-dependent formulation [Eq. (4)]. The equation is consistent with the results herein presented as well as with the Taylor and Yelland (2001) theory, which is in turn consistent with observations from field campaigns at different depths. The validity of the relation should be confirmed with additional assessments spanning a range of water depths. Identifying an adequate depth-dependent relationship will ultimately improve the wind stress representation in our models, and our generalized formula for depths should be regarded as only a starting point.

A better wind stress formulation will also improve the representation of different physical processes involving surface winds. Better wind estimations should be reflected in improved surface-flux estimations, in a more accurate coupling with ocean models that use the wind to derive the stress at the ocean–atmosphere interface, or in improved surge estimations that, for instance, should provide better estimations of storm impacts at coastal locations. From a more applied point of view, the reduced bias in wind simulations should have a direct benefit in the wind-energy industry since the number of offshore wind farms installed over shallow waters has been increasing over the last few years, and this work leads to an improvement for the hub-height winds that are relevant to this application.

Acknowledgments. This manuscript repeats much of the material from a "discussion" paper submitted to *Geosci. Model Dev.* (available at http://www.geosci-model-dev-discuss.net/7/9063/2014/gmdd-7-9063-2014.pdf). After interacting with the chief editor of *Geosci. Model Dev.* we found out that the discussion paper was not suitable for publication in *Geosci. Model Dev.*, mainly because we did not propose a finalized parameterization. The discussion paper has a description of a robust bias and a local solution. This lack of a final parameterization has been addressed in this paper, which includes a generalization of the local solution [Eq. (4)]. The paper also includes several statements on the data and model sensitivities that are in response the *Geosci. Model Dev.* reviewers. We have also benefitted from further reviews in the current journal that led to the testing at the additional site (FINO3), making the findings more robust. The work was supported by project ENE2012-38772-C02-01. Author Dudhia was supported by the National Science Foundation through the National Center for Atmospheric Research and by the Department of Energy through the Wind and Water Power Technology Office (DE-EE0005373).

REFERENCES

Andreas, E. L, L. Mahrt, and D. Vickers, 2012: A new drag relation for aerodynamically rough flow over the ocean. *J. Atmos. Sci.*, **69**, 2520–2537, https://doi.org/10.1175/JAS-D-11-0312.1.

Bretherton, C. S., and S. A. Park, 2009: A new moist turbulence parameterization in the Community Atmosphere Model. *J. Climate*, **22**, 3422–3448, https://doi.org/10.1175/2008JCLI2556.1.

Bryant, K. M., and M. Akbar, 2016: An exploration of wind stress calculation techniques in hurricane storm surge modeling. *J. Mar. Sci. Eng.*, **58**, https://doi.org/10.3390/jmse4030058.

Charnock, H., 1955: Wind stress on a water surface. *Quart. J. Roy. Meteor. Soc.*, **81**, 639–640, https://doi.org/10.1002/qj.49708135027.

DeCosmo, J., K. B. Katsaros, S. D. Smith, R. J. Anderson, W. A. Oost, K. Bumke, and H. Chadwick, 1996: Air–sea exchange of water vapor and sensible heat: The Humidity Exchange Over the Sea (HEXOS) results. *J. Geophys. Res.*, **101**, 12 001–12 016, https://doi.org/10.1029/95JC03796.

Dee, D. P., and Coauthors, 2011: The ERA-Interim reanalysis: Configuration and performance of the data assimilation system. *Quart. J. Roy. Meteor. Soc.*, **137**, 553–597, https://doi.org/10.1002/qj.828.

Donelan, M. A., 1990: Air–sea interaction. *Ocean Engineering Science*, B. LeMehaute and D. M. Hanes, Eds., *The Sea: Ideas and Observations on Progress in the Study of the Seas*, Vol. 9B, John Wiley and Sons, 239–292.

Edson, J. B., and Coauthors, 2013: On the exchange of momentum over the open ocean. *J. Phys. Oceanogr.*, **43**, 1589–1610, https://doi.org/10.1175/JPO-D-12-0173.1.

Fairall, C. W., E. F. Bradley, J. E. Hare, A. A. Grachev, and J. B. Edson, 2003: Bulk parametrization of air–sea fluxes: Updates and verification for the COARE algorithm. *J. Climate*, **16**, 571–591, https://doi.org/10.1175/1520-0442(2003)016<0571:BPOASF>2.0.CO;2.

——, and Coauthors, 2006: Turbulent bulk transfer coefficients and ozone deposition velocity in the International Consortium for Atmospheric Research into Transport and Transformation. *J. Geophys. Res.*, **111**, D23S20, https://doi.org/10.1029/2006JD007597.

Foreman, R. J., and S. Emeis, 2010: Revisiting the definition of the drag coefficient in the marine atmospheric boundary layer. *J. Phys. Oceanogr.*, **40**, 2325–2332, https://doi.org/10.1175/2010JPO4420.1.

Garratt, J. R., 1977: Review of drag coefficients over oceans and continents. *Mon. Wea. Rev.*, **105**, 915–929, https://doi.org/10.1175/1520-0493(1977)105<0915:RODCOO>2.0.CO;2.

Geernaert, G. L., K. B. Katsaros, and K. Richter, 1986: Variation of the drag coefficient and its dependence on sea state. *J. Geophys. Res.*, **91**, 7667–7679, https://doi.org/10.1029/JC091iC06p07667.

——, S. E. Larsen, and F. Hansen, 1987: Measurements of the wind stress, heat flux, and turbulence intensity during storm conditions over the North Sea. *J. Geophys. Res.*, **92**, 13 127–13 139, https://doi.org/10.1029/JC092iC12p13127.

Grachev, A. A., L. Bariteau, C. W. Fairall, J. E. Hare, D. Helming, J. Hueber, and E. K. Lang, 2011: Turbulent fluxes and transfer of trace gases from ship-based measurements during TexAQS 2006. *J. Geophys. Res.*, **116**, D13110, https://doi.org/10.1029/2010JD015502.

Hong, S.-Y., Y. Noh, and J. Dudhia, 2006: A new vertical diffusion package with an explicit treatment of entrainment processes. *Mon. Wea. Rev.*, **134**, 2318–2341, https://doi.org/10.1175/MWR3199.1.

Janssen, J., 1997: Does wind stress depend on sea-state or not?—A statistical error analysis of HEXMAX data. *Bound.-Layer Meteor.*, **83**, 479–503, https://doi.org/10.1023/A:1000336814021.

Jiménez, P. A., J. P. Montávez, E. García-Bustamante, J. Navarro, J. M. Jiménez-Gutiérrez, E. E. Lucio-Eceiza, and J. F. González-Rouco, 2009: Diurnal surface wind variations over complex terrain. *Fis. Tierra*, **21**, 79–91.

——, J. F. González-Rouco, J. Navarro, J. P. Montávez, and E. García-Bustamante, 2010: Quality assurance of surface wind observations from automated weather stations. *J. Atmos. Oceanic Technol.*, **27**, 1101–1122, https://doi.org/10.1175/2010JTECHA1404.1.

——, J. Dudhia, and J. Navarro, 2011a: On the surface wind speed probability density function over complex terrain. *Geophys. Res. Lett.*, **38**, L22803, https://doi.org/10.1029/2011GL049669.

——, J. Vilà-Guerau de Arellano, J. F. González-Rouco, J. Navarro, J. P. Montávez, E. García-Bustamante, and J. Dudhia, 2011b: The effect of heat waves and drought on the surface wind circulations in the northeast of the Iberian Peninsula during the summer of 2003. *J. Climate*, **24**, 5416–5422, https://doi.org/10.1175/2011JCLI4061.1.

——, ——, J. Dudhia, and F. C. Bosveld, 2016: Role of synoptic- and meso-scales on the evolution of the boundary-layer wind profile over a coastal region: The near-coast diurnal acceleration. *Meteor. Atmos. Phys.*, **128**, 39–56, https://doi.org/10.1007/s00703-015-0400-6.

Jones, I., and Y. Toba, 2001: *Wind Stress over the Ocean*. Cambridge University Press, 326 pp.

Kitaigorodskii, S. A., and Y. A. Volkov, 1965: On the roughness parameter of the sea surface and the calculation of momentum flux in the near-water layer of the atmosphere. *Izv. Atmos. Ocean. Phys.*, **1**, 973–988.

Mahrt, L., D. Vickers, J. Howell, J. Hojstrup, J. M. Wilczak, J. Edson, and J. Hare, 1996: Sea surface drag coefficients in the Risø Air Sea Experiment. *J. Geophys. Res.*, **101**, 14 327–14 335, https://doi.org/10.1029/96JC00748.

Nakanishi, M., and H. Niino, 2009: Development of an improved turbulence closure model for the atmospheric boundary layer. *J. Meteor. Soc. Japan*, **87**, 895–912, https://doi.org/10.2151/jmsj.87.895.

Oost, W. A., G. J. Komen, C. M. J. Jacobs, and C. van Ort, 2002: New evidence for a relation between wind stress and wave age from measurements during ASGAMAGE. *Bound.-Layer Meteor.*, **103**, 409–438, https://doi.org/10.1023/A:1014913624535.

Pleim, J. E., 2007: A combined local and nonlocal closure model for the atmospheric boundary layer. Part I: Model description and testing. *J. Appl. Meteor. Climatol.*, **46**, 1384–1395, https://doi.org/10.1175/JAM2539.1.

Skamarock, W. C., J. B. Klemp, J. Dudhia, D. O. Gill, D. M. Barker, W. Wang, and J. G. Powers, 2005: A description of the Advanced Research WRF version 2. NCAR Tech. Note NCAR/TN-468+STR, 88 pp., https://doi.org/10.5065/D6DZ069T.

Smith, S. D., and Coauthors, 1992: Sea surface wind stress and drag coefficients: The HEXOS results. *Bound.-Layer Meteor.*, **60**, 109–142, https://doi.org/10.1007/BF00122064.

Taylor, P. K., and M. J. Yelland, 2001: The dependence of sea surface roughness on the height and steepness of the waves. *J. Phys. Oceanogr.*, **31**, 572–590, https://doi.org/10.1175/1520-0485(2001)031<0572:TDOSSR>2.0.CO;2.

Vickers, D., and L. Mahrt, 2010: Sea-surface roughness lengths in the midlatitude coastal zone. *Quart. J. Roy. Meteor. Soc.*, **136**, 1089–1093, https://doi.org/10.1002/qj.617.

Wilks, D. S., 1995: *Statistical Methods in the Atmospheric Sciences: An Introduction.* Academic Press, 467 pp.

Wu, J., 1982: Wind-stress coefficients over sea surface from breeze to hurricane. *J. Geophys. Res.*, **87**, 9704–9706, https://doi.org/10.1029/JC087iC12p09704.